1 **A methodological roadmap to quantify animal-vectored spatial ecosystem subsidies**

2

3 Diego Ellis-Soto[1,2+], Kristy M. Ferraro[3+], Matteo Rizzuto[4], Emily Briggs[3,5], Julia D. Monk[3], Oswald

4 J. Schmitz[3]

5

6 1 Department of Ecology and Evolutionary Biology, Yale University, New Haven, CT, USA

7 2 Center for Biodiversity and Global Change, Yale University, New Haven, CT, USA

8 3 School of the Environment, Yale University, 370 Prospect Street, New Haven, CT, USA

9 4 Department of Biology, Memorial University of Newfoundland St. John's, Canada

10 5 Department of Anthropology, Yale University, New Haven, CT, USA

11 Corresponding author: diego.ellissoto@yale.edu

12

13 + These authors contributed equally to this work

14

18

19 **Abstract**

20

21 Ecosystems are open systems connected through spatial flows of energy, matter, and nutrients.

22 Predicting and managing ecosystem interdependence requires a rigorous quantitative

23 understanding of the drivers and vectors that connect ecosystems across spatio-temporal

24 scales. Animals act as such vectors when they transport nutrients across landscapes in the form

25 of excreta, egesta, and their own bodies. Here, we introduce a methodological roadmap that

26 combines movement, foraging, and ecosystem ecology to study the effects of animal-vectored

27 nutrient transport on meta-ecosystems. The meta-ecosystem concept — the notion that

28 ecosystems are connected in space and time by flows of energy, matter, and organisms across

29 boundaries — provides a theoretical framework on which to base our understanding of animal-

30 vectored nutrient transport. However, partly due to its high level of abstraction, there are few

31 empirical tests of meta-ecosystem theory, and while we may label animals as important

32 mediators of ecosystem services, we lack predictive inference of their relative roles and impacts

33 on diverse ecosystems. Recently developed technologies and methods — tracking devices,

34 mechanistic movement models, diet reconstruction techniques and remote sensing — have the

35 potential to facilitate the quantification of animal-vectored nutrient flows and increase the

36 predictive power of meta-ecosystem theory. Understanding the mechanisms by which animals

37 shape ecosystem dynamics may be important for ongoing conservation, rewilding, and

38 restoration initiatives around the world, and for more accurate models of ecosystem nutrient

39 budgets. We provide conceptual examples that show how our proposed integration of

40 methodologies could help investigate ecosystem impacts of animal movement. We conclude by

41 describing practical applications to understanding cross-ecosystem contributions of animals on

42 the move.

43

Introduction

Ecosystems and animal nutrient cycling

Flows of energy, nutrients, matter, and organisms crisscross landscapes worldwide, connecting intrinsically open ecosystems over space and time. The advancement of meta-ecosystem theory (Loreau *et al.* 2003; Leroux & Loreau 2008; Massol *et al.* 2011; Marleau *et al.* 2014) has aided our understanding of the influence of these spatial exchanges in both donor and recipient ecosystem functioning (Gounand *et al.* 2018b). Classic ecosystem theory holds that the spatial flow of organic and inorganic matter from source to recipient locations is largely passive, coming for example from *in situ* weathering of parent geological material, release from riverine sediments, wind-born dust, or rain-driven and snowmelt-driven run-off (Chapin *et al.* 2012). Nevertheless, there is growing appreciation that ecosystems also receive subsidies via animal movement (Vanni, 2002; Atkinson, Capps, Rugenski, & Vanni, 2017; Schmitz et al., 2018; Mcinturf, Pollack, Yang, & Spiegel, 2019). Such movement can result in an influx of new prey or predators to recipient locations, pulses of animal-transported nutrients in dung and urine, or the accumulation of organic matter via decomposition of carcasses deposited in recipient locations (henceforth, animal-vectored subsidies; Earl & Zollner 2017; Mcinturf *et al.* 2019). Whenever biotic—such as animal-vectored subsidies—or abiotic processes influence the structure and functioning of ecosystems, they are deemed ecosystem controls (Weathers *et al.* 2012). Theory predicts that animals can exert top-down control on ecosystems via subsidies, the magnitude of which could sometimes be equal to bottom-up (Leroux & Loreau, 2008; Allen & Wesner, 2016).

Increasingly, migratory populations of large bodied species are recognized for playing an especially important role as landscape-scale vectors of ecosystem subsidies (Bauer & Hoye 2014). Yet at the same time, across the globe, their populations are in decline (Wilcove & Wikelski 2008; Dirzo *et al.* 2014) and their movement is increasingly constrained by human activities (Tucker *et al.* 2018). The implications of such effects on top-down control over ecosystem functioning at broad spatial scales remain uncertain, but estimates suggest they can be substantial (Doughty *et al.* 2016). Hence, an important avenue of new research in ecosystem ecology is empirically resolving the relative importance of animal-vectored vs. passive subsides on ecosystem functioning. We are at an opportune scientific and technical juncture to begin synthesizing advances made in disparate fields.

78   The empirical challenge in understanding and attributing how much control animals exert over
79   ecosystem functioning is to quantify spatial flows of different kinds of animal-vectored subsidies
80   (i.e. excretion, egestion, carcass deposition, reproductive material). While theory is in place to
81   identify the different components that need measuring to obtain a coherent understanding of this
82   phenomenon (Leroux & Loreau, 2008; Earl & Zollner, 2017; Gounand et al. 2018; Schmitz et al.,
83   2018), it remains largely conceptual and offers few insights into how to operationalize empirical
84   measurement. Here, we address this limitation by offering a methodological road map that
85   discusses the various measurements that need to be integrated to develop a coherent picture of
86   the quantitative effects of animals on nutrient dynamics across ecosystems. There is now
87   unprecedented ability to characterize functional and structural properties of ecosystems
88   including topography, vegetation community composition, and habitat structure across vast
89   spaces (Bergen *et al.* 2009; Pettorelli *et al.* 2018). Likewise, movements of a wide range of
90   animal species can be monitored remotely (Kays, Crofoot, Jetz, & Wikelski, 2015; Wilmers et
91   al., 2015a), which can facilitate quantification of the net effects of animals on nutrient and
92   material transport. New DNA-based and isotopic analyses can resolve dietary nutrient sources.
93   Additionally, these nutrient sources and fates can be mapped spatially using nutrient distribution
94   modeling (West et al. 2010; Sitters *et al.* 2015; Leroux *et al.* 2017). While ripe for integration,
95   these methods and technologies continue to be deployed separately in research that examines
96   different components of animal movement and resource use within ecosystems. We show here
97   how these different methods can be used jointly to give a coherent, theory-driven understanding
98   of the ecosystem consequences of animal-vectored nutrient flows across landscapes.
99
100   **Materials and Methods**
101
102   **Meta-ecosystem models to understand animal-vectored subsidies**
103
104   The series of measurements we discuss are motivated by ecological theory on meta-ecosystem
105   dynamics. A multitrophic version of such an ecosystem model can be used to consider how
106   internal dynamics of ecosystems are connected by regional flows of materials and organisms
107   between the ecosystems (Marleau *et al.* 2014). To identify the processes that need to be
108   measured, we consider a model configured as a four trophic level food chain (Fig. 1), which
109   describes the dynamics of a single abiotic nutrient or element (N), a plant (P), a herbivore (H),
110   and a carnivore (C) within and between i local ecosystems that together create the meta-
111   ecosystem. This structure is intended for simple illustrative purposes to show how to relate the

112 dynamical systems model to the salient ecosystem and spatial processes that need to be
113 measured. The model can be made more complex by considering multiple nutrients to make it
114 stoichiometrically explicit (Leroux *et al.* 2012; Cherif & Loreau 2013) as well as multiple species
115 among trophic levels (McCann *et al.* 2005). Such granularity is beyond the scope of this paper.
116 Instead, we use this theoretical framework specifically to identify salient processes (and inherent
117 variables) that need to be measured to obtain a quantitative understanding the role of animals in
118 connecting and shaping the structure and functioning of local ecosystems across spatial scales.
119 The model reveals two salient processes that need to be considered: trophic interactions and
120 nutrient translocation and deposition. These two processes can be subdivided into five more
121 finely resolvable spatial components (Fig.1) that require detailed measurement. Hence, our
122 roadmap focuses on measuring these five components.

123

124 Trophic interactions within ecosystem i determine nutrient uptake and assimilation by
125 herbivores and carnivores (Fig. 1) that may vary in size, and habitat structure within an
126 ecosystem determines species spatial occurrences and the nature of their interactions (Schmitz
127 et al. 2017). Thus, an accounting of animal spatial interactions will require analysis of: (1) the
128 spatial extent and spatial grain size for analysis of the focal animal species and their
129 interdependent predators or prey/resources (i.e., spatial trophic food chain structure) in relation
130 to (2) the habitat structure within and between source and recipient local ecosystems. Moreover,
131 animals can be selective in their choice of resources, necessitating further spatial analyses of
132 (3) the resources selected by animals in source and recipient locations. Nutrient translocation
133 and deposition in ecosystems will depend on (4) the movement rates and directional spatial
134 flows of animal species and animal-vectored nutrients, and (5) the amounts and spatial
135 deposition rate of animal transported nutrients or materials, which can include the animals' own
136 body mass, waste products, reproductive material, and dispatched prey. Each of these
137 components can be measured with its own set of technologies (Fig. 2). We next provide a brief
138 review of these tools and of their potential use in the context of measuring animal-vectored
139 subsidies.

140

141 ***(1) Spatial trophic structure***
142 The first step to understanding how animal movement shapes ecosystems is to describe the
143 geographic domain over which focal animals roam and their trophic position within food chains,
144 including the scope of interactions with predators and resources (Fig. 2). These factors will
145 determine the geographic area and spatial grain of interest, the animals' habitat domain within

146 that area, and any ecosystem effects the animal could have within said domain through
147 cascading impacts on associated food webs. The habitat domain is the spatial extent of habitat
148 space used within a species' broader home range that is relevant to interspecific interactions,
149 e.g., areas used for foraging or avoiding predation (Schmitz *et al.* 2017).

150

151 Characterizing the spatial grains at which animals interact with other species and their
152 environment is crucial to understanding their distributions. Animal movement can be described
153 at fine spatial scales (e.g. responses to environmental resources such as foraging [see section
154 3]) or at coarser scales, such as their broad home range (introduced in section 4) (Mertes *et al.*
155 2020). Fine and coarse spatial grains have been termed "response grain" and "occupancy
156 grains", respectively (Mertes *et al.* 2020). To quantify an animal's response grain, first passage
157 time analysis can be employed. These are defined as the time it takes an animal to cross a
158 circle with a defined radius -- and as such scale dependent -- and can quantify the time duration
159 of an individual animal present within such a circle (Fauchald & Tveraa 2003). First passage
160 time allows estimating the spatial scale at which an individual animal focuses its search efforts
161 (i.e. by plotting variance in first passage time against the spatial scale, Fauchald & Tveraa 2003,
162 Fig. 2 bottom left panel). As such, hierarchical scales of animal habitat selection (Johnson 1980;
163 Mertes & Jetz 2017; Mertes *et al.* 2020) should drive the spatial resolution of remote sensing
164 products selected for analysis, not the other way around. This is especially relevant for animal
165 movement data, which are typically measured at finer spatio-temporal resolutions than data
166 from remotely sensed imagery (Remelgado *et al.* 2017, 2019). The habitat domain can be
167 measured using movement data by tracked individuals across a landscape, to calculate an
168 animals utilization distribution and probabilities of spatial locations associated with foraging and
169 migration behaviour across a landscape (Schmitz et al. 2017). A three-dimensional utilization
170 distribution could be estimated if vertical movements are tracked, e.g. movement in forest
171 canopies (McLean *et al.* 2016).

172

173 Species interactions can alter animal movement behaviour, which can in turn impact ecosystem
174 nutrient dynamics (Schmitz, Hawlena, & Trussell, 2010; Schmitz et al., 2018). Hence
175 consideration of the amount and spatial domain of animal vectored subsidies needs to consider
176 species embeddedness within food chains. Moreover, such consideration will enhance the
177 appreciation that animal vectored subsidies can trigger the rearrangement of food chains or
178 initiate novel trophic interactions (Montagano *et al.* 2019). Generally in this context, primary
179 producers have a trophic position of 1, primary consumers have a trophic position of 2,

180 secondary consumers have a trophic position of 3, and so on (Leroux & Loreau 2012). Yet there
181 are many animals that occupy trophic positions between these discrete designations. For
182 example, an omnivore may consume mostly primary consumers, but also some secondary
183 consumers and therefore have a trophic position between 2 and 3 (Kelson et al 2020). We
184 discuss how stable isotopes may be used to determine trophic position in section 3, which is
185 important to resolve the nature and source of nutrients (e.g. largely plant-based vs. largely
186 animal-based) that comprise subsidies (see section 3, Kelson et al. 2020).
187
188 *(2) Habitat structure within and between source and recipient locations*
189
190 Habitat structure and topographic features, within and between source and recipient locations,
191 shape animal movement and nutrient transport within habitat domains (Leroux & Loreau, 2008;
192 Gounand, Little, Harvey, & Altermatt, 2018; Schmitz et al., 2018). A spatially accurate
193 characterization of these fundamental ecosystem attributes is key to understanding why, how,
194 and where animals move over the landscape (Fig. 2). Earth observation via satellite, airborne,
195 or drone imagery provides an important basis for developing such a characterization (Allan *et al.*
196 2018; Pettorelli *et al.* 2018). Remotely sensed landcover maps (i.e. forest, grassland, urban) can
197 be used to delineate ecosystem boundaries and assess how these change through time.
198 Advances of LiDAR (Light Detection and Ranging) make it possible to characterize vertical
199 habitat structure and above-ground vegetation biomass within and across ecosystem
200 boundaries. Furthermore, ecosystem productivity can be remotely measured and represented
201 as vegetation indices (de Araujo Barbosa *et al.* 2015; Pettorelli *et al.* 2018). Topographic
202 products, such as slope and topographic ruggedness (Amatulli *et al.* 2018), can resolve passive
203 abiotic flow pathways to pinpoint where nutrients may end up on the landscape (e.g., flow down
204 concave and into convex surfaces; Lindeman, 1942; Leroux & Loreau, 2008). Finally, LiDAR
205 estimates are becoming available from the Global Ecosystem Dynamics Investigation (GEDI)
206 mounted on the International Space Station, which measures forest structure and above-ground
207 biomass density across the globe (Hancock *et al.* 2019)
208
209 More finely resolved structure can be obtained within habitats using hyperspectral technologies
210 to collect hundreds of bands across the electromagnetic spectrum which distinguish unique
211 'fingerprints', referred to as spectral signatures for different kind of environmental features
212 (Stuart *et al.* 2019). Such spectral signatures can be related to spatial patterns in plant
213 functional diversity, vegetation elemental composition, and plant density (Knyazikhin *et al.* 2013;

214   Jetz *et al.* 2016; Schneider *et al.* 2017; Durán *et al.* 2019). Further, endmember extraction from

215   multispectral imagery can be used to extract information on subpixel features, e.g., to identify

216   signatures of water availability and abundance (Xie *et al.* 2016) .

217

218   Remotely sensed environmental products have different pixel resolution, commonly referred to

219   as 'grain size'. Accessing and utilizing a plethora of remote sensing products is facilitated

220   through geoprocessing tools such as Google Earth Engine, the Movebank Env-Data system,

221   and the getspatialdata package (Pettorelli *et al.* 2014; Clark *et al.* 2016; Wegmann 2017). We

222   list a collection of remote sensing products available to study ecosystem features across source

223   and recipient locations in Table 1. Regardless of the product used, coherent understanding

224   requires a grain size that aligns with the grain size of measurement of animal movement.

225

226   ***(3) Resources available to and selected by animals in source and recipient locations***

227

228   Characterization of species habitat domains and structure can next be used to determine why

229   animals move where they do, and what resources they use in source and recipient locations

230   (Fig. 2). This can be accomplished using resource selection functions (RSF; Boyce *et al.* 2002)

231   and step selection functions (SSF; Fortin *et al.* 2005). Generally, these functions associate

232   environmental variables with locations used by individual animals and compare these with

233   randomly generated points representing locations available to, but not used by, them (Michelot

234   *et al.* 2019). Both methods estimate the probability of animal presence as a function of

235   environmental covariates. SSF can be used further to predict future movement paths of animals,

236   while RSF predicts spatial patterns of species occurrences over spatio-temporal scales

237   (Michelot *et al.* 2019). Parameters from SSF can highlight whether animals avoid or are

238   attracted to certain landscape features or resources. For example, SSF analysis reveals that in

239   Etosha National Park, Namibia, elephants avoided areas with high tree biomass and were

240   attracted to water sources and grassland patches with long term patterns of productivity

241   (Tsalyuk *et al.* 2019). This could indicate that waterholes and grasslands receive more animal-

242   vectored subsidies from elephants when compared to steep areas or dense forests. Such

243   behavioural information would improve mechanistic predictions of nutrient redistribution by

244   these wide-ranging megafauna which are known to play a large effect on regional carbon

245   budgets (Berzaghi *et al.* 2018).

246

247   Resource selection is a hierarchical process (Courbin et al. 2013). While RSF and SSF are
248   broad-scale measures of animal movement and habitat use, more finely resolved measures are
249   needed to understand which food items are used by animals and their nutritional values within
250   different locations. This understanding of animal food consumption and eventual processing and
251   deposition (in body material, or as urine and fecal matter) can provide an understanding of
252   where and how nutrients removed from donor ecosystems end up in recipient ecosystems.
253   Additionally, the identity of consumed resources directly impacts the quantity and quality of
254   nutrients deposited by animals (Subalusky & Post 2018).

255

256   Traditionally, dietary analyses have been performed based on physical dissection and
257   microhistological analyses of stomach contents and fecal matter (Holechek et al., 1982, Joly,
258   2018). These methods, however, often require either opportunistic sampling of carcasses or
259   destructive harvesting of live animals. DNA-metabarcoding provides an alternative, as it allows
260   for the identification of materials consumed using fecal matter alone (Kartzinel *et al.* 2015; see
261   Deagle et al., 2019 for an overview of DNA-metabarcoding methods). DNA-metabarcoding can
262   shed important insights into the trophic ecology of source and recipient sites, and how
263   consumption, and thus acquisition and transport of nutrients, can change in time and space
264   (Pansu *et al.* 2019). For example, Atkins et al. (2019) combined GPS tracking data of bushbuck
265   (*Tragelaphus sylvaticus*) with DNA-metabarcoding of fecal samples to show that herbivores
266   occupy new habitats and forage on novel food items after extirpation of their predators.
267   Bushbuck presence further changed plant community composition (demonstrated by comparing
268   plant composition in exclosure and control plots) (Atkins *et al.* 2019). A playback experiment of
269   predator sounds was able to revert bushbuck behaviour as they perceived predation risk (Atkins
270   *et al.* 2019).

271

272   Stable isotopes, such as δ^{15}N, δ^{13}C, and δ^{18}O, are also powerful tools in elucidating the trophic
273   position (Ben-David et al., 2012), diet, and foraging location of a focal species in a non-invasive
274   manner (Newsome *et al.* 2010; Kristensen *et al.* 2011). In general animals are enriched by ~3‰
275   of nitrogen and ~1‰ of carbon compared to what they eat, providing an estimate of trophic
276   position (Post 2002). Therefore, trophic position can be discerned by using the isotopic
277   signature (i.e. δ^{15}N) of the consumer, of the ecosystem's primary producers, and a
278   discrimination factor for the change in δ^{15}N enrichment between the ecosystem's trophic levels
279   (Kelson *et al.* 2020). Using stable isotopes could also be a cost-effective way to identify the
280   correct primers when conducting DNA-metabarcoding. For example, while white-tailed deer are

281 primarily herbivores, there is some evidence that they sometimes consume animal matter (Ellis-
282 Felege *et al.* 2008). If stable isotopes revealed that deer have an omnivorous diet, DNA-
283 metabarcoding could be used to discern exactly what animal material they consumed.

284

285 Stable isotopes can also be used to arrive at approximate estimates of diet. The isotopic
286 signatures of food items (for example, C3 and C4 plants) often vary from one another.
287 Therefore, examining the isotopic signature in bone, tooth, or feces has shown a successful
288 method of coarsely understanding diet (Ben-David & Flaherty 2012). We recommend using
289 stable isotopes to determine diet if DNA-metabarcoding is not financially possible, when using
290 samples that have degraded and DNA-metabarcoding is no longer possible, or when a broad
291 understanding of diet is sufficient for the question at hand For an extensive overview of using
292 stable isotopes for ecological research, see Ben-David & Flaherty (2012), Hobson et al., (2019),
293 and West *et al.* (2010).

294

295 ***(4) The movement rates and directional patterns of animal species and subsequently***
296 ***translocated nutrients***

297

298 Animals can transport nutrients along and against biophysical gradients (Earl & Zollner, 2017;
299 Mcinturf et al., 2019). Therefore, an understanding of animal movements will elucidate the
300 nature and scale of consequent nutrient transfer (Fig. 2). Patterns of animal movement are
301 directly related to the degree of connectivity (c_{ij}, Fig. 1) among local ecosystems as well as the
302 movement rates of the animals (d_H, d_C, Fig. 1), which depend on the topography of the
303 biophysical gradient. Advances in animal tracking technologies – dubbed biologging – offer
304 possibilities to study internal (e.g., physiology, metabolism, reproduction) and external (e.g.,
305 social, environmental) drivers of animal movement (Nathan *et al.* 2008). Biologging enables
306 quantification of the space-use and resource requirements of animals (Kays *et al.* 2015; Hays *et*
307 *al.* 2019). The frequency with which animals visit certain areas (e.g., waterholes, fruit bearing
308 tree, latrines) can be estimated via first passage times and recursive analysis (Mahoney &
309 Young 2017; Bracis *et al.* 2018; Mertes *et al.* 2020).

310

311 Migrations are among the greatest examples of animal movement. Extensive research has
312 explored their direction, length, and drivers (Dechmann *et al.* 2017; Somveille *et al.* 2018, 2019).
313 Locations of an animal's track can be classified into specific movement strategies (i.e. disperser,
314 migrator, nomad, central place forager) by segmentation methods (Bastille-Rousseau *et al.*

315 2016; Edelhoff *et al.* 2016), thus setting the stage for further analysis. Fine-scale animal
316 behaviour (i.e. foraging, rest, travel) can be resolved in GPS data using behavioural change
317 point analysis, expected-maximum binary clustering methods (Garriga *et al.* 2016), and state-
318 space models (Patterson *et al.* 2008). A promising approach combining state-space and
319 continuous time correlated random walk models (Michelot & Blackwell 2019) allows estimating
320 behavioural states when using tracking data that are not sampled at regular time intervals,
321 which is a common occurrence with biologging data.

322

323 Modern biologging tags are comprised of GPS units, accelerometers, and additional on-board
324 sensors. Accelerometers estimate change in velocity of body postures over time and can
325 classify behavioural states of wild animals, including hunting, killing, resting (Brown *et al.* 2013;
326 Williams *et al.* 2014), and even scent marking (Bidder *et al.* 2020). Accelerometers also allow
327 quantifying energy expenditure of animals and of specific behaviours. Common methods for
328 such energy expenditure are two closely linked metrics; Overall Dynamic Body acceleration
329 (ODBA) and Vectorized sum of the Dynamic Body Acceleration (VeDBA) (Wilson *et al.* 2006,
330 2020). We refer to Joo, Boone, Clay, & Patrick, (2019) for a review on animal movement
331 analysis.

332

333 Movement ecology increasingly studies fine scale behaviours such as foraging or sociality
334 (Strandburg-Peshkin *et al.* 2015; Bennison *et al.* 2018) that can determine fine scale spatial
335 heterogeneity in nutrient release, a process not yet considered in the current literature on
336 animal-vectored subsidies (Gounand *et al.* 2018b). At the same time, movement ecology rarely
337 quantifies the scale, scope, and magnitude of animal-mediated nutrient transfers.

338

339 (*5) The amounts and deposition rate of animal transported nutrients or material*

340

341 Remote sensing offers quantitative measures of ecosystem structure at broad geographic
342 scales. Collecting environmental data in the field provides detailed information that is essential
343 and complementary to remote sensing to understand how local microclimate influences
344 ecosystem dynamics and the distribution of animals and the resources they consume
345 (Zellweger *et al.* 2018) (Fig. 2, right panel). Local observations identify how trophic interactions
346 and community structure vary across habitats and environmental gradients. For example, one
347 could measure a site's microtopography (slope, elevation, roughness), surrounding vegetation
348 type and cover. The development of methods to account for such micro-environmental variation

349   is necessary to facilitate realistic representations of environmental conditions experienced by
350   organisms. Downscaled remote sensing products show promise in providing such fine spatial
351   detail (Maclean *et al.* 2019; Maclean 2020) and, once overlaid with animal locations, enable
352   identification of habitats that are source and recipient locations for animal-vectored nutrient
353   subsidies.

354

355   Animal vectored subsidies involve several processes, including consumption, excretion,
356   egestion, and deposition of carcasses and parturition material (McSherry & Ritchie 2013;
357   Subalusky & Post 2018; Wenger *et al.* 2019). For example in the Maasai Mara National Park
358   Reserve, Kenya, every day Hippopotamus egest approximately 36 tons of wet biomass
359   consumed in terrestrial ecosystems into the Mara river, approximately 15 % of the dissolved
360   organic carbon loading from the upstream catchment (Subalusky *et al.* 2015). Also in the Mara,
361   mass drowning of wildebeest contributes ~18% of the total dissolved organic carbon to the river
362   ecosystem (Subalusky *et al.* 2017).

363

364   Standard biogeochemical methods, which include analyses that quantify elemental composition
365   of materials, can be used to characterize the stoichiometry and total nutritional composition of
366   food items (Vanni et al., 2002). Additionally, these methods can assess nutrient quality and
367   quantity of animal-deposited material (e.g. egesta, excreta, carcasses) as well as the magnitude
368   of nutrient influx into the surrounding environment through *in situ* measurement of various soil
369   and plant properties (e.g., pH, soil texture, plant community composition, soil and plant nutrient
370   content) at sites of animal activity (i.e. see Bump et al., 2009, Risch *et al.* 2020). Finally, given
371   that stable isotope that come from animal tissues and excreta are isotopically enriched
372   compared to their diet, enriched plant and soil materials surrounding the deposition can indicate
373   deposition and use of animal-vectorized subsidies (Bump et al 2009a). Such enrichment may
374   also help parse out passive from active subsidy input.

375

376   The tracing and mapping of spatial nutrient flows and deposition can be aided by using
377   stoichiometric distribution models (StDMs). Such models predict the geospatial distribution of
378   nutrients in forage items (Leroux *et al.* 2017). Similar to a species distribution model and point
379   Poisson process models, a resource – in this case a forage item's nutrient content, either
380   absolute (g/m^2; i.e. quantity) or relative (carbon:nitrogen ratio; i.e. quality) – can be defined as
381   the abundance of a given nutrient (nitrogen, phosphorus or carbon) in location x_i which is
382   predicted by a vector of environmental covariates $z_{(x_i)}$, their coefficients β_i, and an error term ε.

383   StDMs map the distribution of nutrients in ways that can be overlaid with animal spatial habitat
384   domains, to reveal how animals respond to spatial variation in resource distribution across a
385   landscape (Leroux *et al.* 2017) and may create microsites of heterogeneity where subsidies are
386   transported against stoichiometric gradients in the broader landscape.
387

388   **From diverse data sources, to a coherent message - A road map for integrating methods**

389   The current technological and methodological juncture allows us to go beyond understanding
390   the drivers of animal movement. We now have the tools to enhance our understanding of the
391   ecosystem-wide consequences of animal movements, generating inference on the timing,
392   directionality, and magnitude of animal mediated subsidies on both donor and recipient
393   ecosystems. Our road map identifies five steps needed to develop such a coherent picture and
394   is presented in Figure 2. We illustrate the value of this road map with two case studies, one of a
395   herbivore and one of a top predator, discussing how methods from these five steps can be
396   integrated to understand how animals on the move influence their ecosystems at fine scales.
397

398   *Case Studies*
399   **Measuring nutrient loading by Galapagos tortoises during their seasonal migration**
400   Galapagos tortoises (*Chelonoidis porteri*) are ecosystem engineers due to their seed dispersal
401   abilities, trampling of vegetation, and transport of nutrients (Gibbs *et al.* 2010; Blake *et al.* 2012;
402   Ellis Soto 2020). Coupling tortoise tracking data with remotely sensed NDVI has identified that
403   giant tortoises undergo seasonally recurring migrations in response to averages of long-term
404   environmental conditions (Bastille-Rousseau *et al.* 2019). Behavioural observations revealed
405   that tortoises preferentially feed on an agricultural crop (guava, *Psidium guajava*) when
406   migrating from higher to lower elevation areas (Blake *et al.* 2015). By preferentially feeding on
407   guava in agricultural areas, tortoises translocate guava seeds and nutrients into other habitats
408   during their downslope migration, resulting in the spread of guava as an invasive species and
409   posing a challenge to the maintenance of natural plant communities in Galapagos National Park
410   (Ellis-Soto *et al.* 2017). The distribution of guava has been mapped through local vegetation
411   sampling plots and drone and remote sensing imagery (Rivas-Torres *et al.* 2018; Laso *et al.*
412   2019). Coupling tortoise movement patterns, resource selection, and habitat structure makes it
413   possible to quantify giant tortoise vectored nutrient transfer in Santa Cruz Island, Galapagos.

414   Santa Cruz Island shows a distinct zonation of vegetation. Dry xerothermic plants dominate the
415   low elevations of the national park, with rainfall and the presence of introduced species (e.g.,
416   guava) increasing with elevation (Itow 2003). During their downslope migration, adult tortoises
417   can migrate from agricultural areas at higher elevations into the lowlands of the Galapagos
418   National Park (identified through net square displacement, Suppl. Material 1). Overlapping
419   home ranges (Winner *et al.* 2018) of tagged tortoises located in the lowlands inside the national
420   park can reveal core areas of tortoise utilization distributions, providing a picture of spatial
421   trophic structure. Using this core area, a stratified sampling of surrounding vegetation, soil
422   samples, and description of microtopography can help understand nutrient composition,
423   microbial activity and abiotic properties of selected areas in an attempt to further characterize
424   habitat structure. Such measurements could be compared with samples obtained in areas
425   where tortoises are absent, serving as a control plot (i.e. via exclosures or randomly selecting
426   points outside the tortoise core area) to further isolate animal impacts on biogeochemical cycles
427   and ecosystem fluxes.

428   Given their different photosynthetic pathways (C3 and CAM, respectively) guava likely contains
429   a different isotopic signature (Sage & Zhu 2011) than the tortoises' most-consumed xerothermic
430   plant at lower elevations of the National Park, the *Opuntia echios* cacti. Thus, stable isotope
431   analysis of fecal matter containing guava could disentangle contributions by tortoises during
432   their migrations from a donor ecosystem (agricultural areas) to a recipient ecosystem (lowlands
433   of the Galapagos National Park) and make spatially explicit predictions of this animal-vectored
434   nutrient flux. Finally, all of these measures can be combined to develop a nutrient budget for the
435   lowland ecosystem of the Galapagos National Park and include the downslope migration of *C.*
436   *porteri* as the mechanism for vectored subsidy (Fig. 3, Fig. 4). Such nutrient ecosystem budgets
437   often attempt to quantify the flows of nutrients through different pools providing an
438   understanding of how these flows may impact ecosystem functioning (Loreau & Holt 2004).
439   Coupling an assessment of nutrient loading with past and present tortoise population numbers
440   could provide a baseline for ongoing conservation initiatives aimed at restoring degraded island
441   habitats by reintroducing giant tortoises to act as ecosystem engineers (Gibbs *et al.* 2010;
442   Hunter *et al.* 2020). We provide the necessary code to replicate steps detailed in this conceptual
443   tortoise example (Suppl. Material 1).

444   **Quantifying how *Canis lupus* creates landscape heterogeneity through prey hunting and**
445   **killing**
446

447   Predators can have profound cascading impacts on ecosystem nutrient dynamics mediated by

448   their effects on prey mortality and space use (Fig. 5). For example, the hunting behaviour of

449   wolves (*Canis lupus*) and the subsequent deposition of prey carcasses may create nutrient

450   hotspots across a landscape, creating heterogeneity in nutrient distribution as carcasses

451   decompose at sites with high rates of predation (Bump *et al.* 2009a; Joseph *et al.* 2009). To

452   explore this, a recursive analysis (Bracis *et al.* 2018) based on how often animals return to

453   specific landscape areas defined by a determined circular radii — which could be chosen based

454   on grain sizes identified from First Passage Times (Mertes *et al.* 2020) — display where and

455   how collared wolves revisit areas in their range. Coupling accelerometer and animal location

456   data can identify hunting, eating, and killing by predators in the wild through behavioural

457   classification and ground-truthing GPS clusters at presumed kill sites (Williams *et al.* 2014;

458   Wang *et al.* 2015). These methodologies can pinpoint the exact coordinates and time of hunting

459   and killing events and therefore quantify the movement of the nutrients through these

460   processes. Once a carcass's presence is identified, camera traps can provide insight into how

461   the predation behaviours of top predators may have cascading impacts on subsidizing

462   scavengers and invertebrates (Perrig *et al.* 2017; Cunningham *et al.* 2018).

463

464   Using a stratified sampling scheme of plant and soil characteristics, it is also possible to quantify

465   the nutrients deposited by the carcasses, explore the spatial diffusion of those nutrients, and

466   estimate how long those nutrients stay in the local system before leaching away or being

467   scavenged. These sites can be compared to measurements collected in randomly selected

468   points, which may serve as a control treatment. Assessing the plant community composition and

469   cover will help identify whether killing behaviour of predators leads to changes in plant

470   composition, while soil samples collected below carcasses can be used to compare microbial

471   activity and nutrient availability between carcass and control sites (Metcalf *et al.* 2016; Risch *et*

472   *al.* 2020). Both total soil and plant nutrient concentration as well as enriched δ^{15}N in plant and

473   soil samples can be used to identify and quantify the impact of this animal vectorized subsidy

474   (Bump *et al.* 2009b; Holtgrieve *et al.* 2009; Barton *et al.* 2016). This conceptual study design

475   highlights how predators could concentrate nutrients at kill sites, contributing to landscape

476   heterogeneity with potential knock-on effects on scavenger and plant community distribution.

477   Such knowledge is key for understanding the ecosystem consequences of predator loss (Ripple

478   *et al.* 2014).

479

480   **Moving forward: Future Directions**

481

482   We have illustrated how individual studies may productively integrate disparate fields and tools
483   to address specific questions about animal-vectored nutrient subsidies within a study system.
484   These disciplines and methodologies can be united to address larger questions about animals
485   and nutrient transport in diverse systems and at multiple scales. Below, we identify the next
486   frontiers in ecological research, which can be resolved through synergistic research linking
487   animal movement and nutrient transport.

488

489   **Improve tracing and mapping of animal vectorized subsidies**

490

491   We see opportunities to improve predictions of animal vectored subsidies based on advances of
492   Species Distribution Modeling (SDM) such as incorporating a priori expert knowledge (Merow *et*
493   *al.* 2016) and joint species distribution modeling (jSDM) (Pollock *et al.* 2014). Such expert
494   knowledge can represent species geographic ranges or species specific elevational ranges as
495   known from field guides. Expert knowledge could enter StDM's in the form of a statistical offset
496   which has been shown to improve model predictions from SDM's (Ellis-Soto *et al.* n.d.; Merow
497   *et al.* 2016). Such offset is independent of the predictor variable (nutrient quantity or quality) and
498   would provide *a priori* expectations of how resources are distributed across a study region
499   rather than assuming an equal likelihood for each cell in a landscape. StDMs could also
500   incorporate soil nutrient maps derived from coarse scale remote sensing (soilgrids database) as
501   an offset reflecting the a priori expectation of a nutrient concentration in a cell. We refer to
502   Merow, Wilson, & Jetz, (2017) for specifics about deploying offsets in logistic regression, but the
503   motivation is that expert information can provide estimates that are complementary to point
504   estimates that could predict nutrient quantity (g/m^2) or nutrient ratios (C:N).

505

506   jSDMs predict spatial occurrences of entire communities of species, rather than distributions of
507   single species, as in SDM (Pollock *et al.* 2014). StDMs could be similarly extended to consider
508   the distribution of multiple individual nutrients (not just their ratios). Particularly, we see potential
509   in adapting jSDM developments from Generalized joint attribute modelling (Clark *et al.* 2017),
510   Bayesian Ordination and Regression Analysis of Multivariate Abundance Data (Hui 2016), and
511   Spatial factor analysis (Thorson *et al.* 2015) to develop joint StDM. Such jStDM could be
512   overlapped with autocorrelated kernel density estimators (Fleming *et al.* 2015) to investigate
513   how animal space use relates to spatial stoichiometry.

514

515   We see potential in building upon mechanistic models of animal movement and seed and
516   nutrient dispersal to map the distribution and magnitude of animal vectored subsidies (Bampoh
517   *et al.* 2019; Kleyheeg *et al.* 2019; van Toor *et al.* 2019). These models couple animal movement
518   and gut retention with remotely sensed land cover information to create spatially explicit maps of
519   nutrient dispersal. Such models have provided insights about how extinct and extant animals
520   have influenced nutrient translocations at coarse spatial scales across the globe (Doughty *et al.*
521   2016; Doughty 2017). These estimates could be refined by incorporating movement models
522   such as allometric random walks (Hirt *et al.* 2018) and individual based movement models
523   (Bampoh *et al.* 2019), rather than coarser lateral diffusion movement models which have
524   hitherto been used.
525
526   **Estimating animal-mediated nutrient translocation within a home range**
527
528   Core areas where individuals within groups or populations might have strongest animal-
529   vectorized subsidies effects can be identified using home range overlap indices between
530   individuals. Such overlap indices may be simple convex hulls around individual home ranges to
531   describe population ranges or more sophisticated utilization distributions based on bias-
532   corrected Bhattacharyya coefficient as shown by Winner et al., (2018). RSFs of individuals with
533   overlapping home ranges could reflect how these animals utilize resources across long-term
534   timescales.
535
536   Behavioural pattern identification could characterize a suite of animal behaviours within home
537   ranges (e.g., forage, rest, fight, prey capture; Kie *et al.* 2010) to identify how animals transport
538   nutrients at shorter timescales (Fig. 3). Revisitation and accelerometer analysis hold promise to
539   identify feeding sites, scent marking sites or latrines (Bracis *et al.* 2018; Bidder *et al.* 2020). High
540   urine concentration at latrines could influence plant communities, soil nutrient loads, and
541   microbial communities, constituting a nutrient hotspot. Other methods estimate nest locations
542   and reproductive output from telemetry data (Picardi *et al.* 2019; Bidder *et al.* 2020). Such
543   behavioural identification can identify where animals assimilate or excrete resources and under
544   which conditions animals act as nutrient sources (bring more nutrients in than they consume,
545   i.e. high urine concentration at latrines or high offspring mortality at nests) or sinks (have a
546   negative net effect on nutrient concentrations at the site). Calculating integrated step selection
547   functions (Avgar *et al.* 2016) using exclusively animal locations that were associated with
548   foraging behaviour (Nathan *et al.* 2012) could identify such nutrient sources. Habitat selection

549 could be explored at fine detail by using drones to create study-site specific landcover maps
550 (Strandburg-Peshkin *et al.* 2017).

551

552 **Animal-vectored subsidies in the Anthropocene**

553

554 In human-modified landscapes, animals find themselves crossing a matrix of fragmented
555 habitats and human pressures (i.e. population density, infrastructure and agricultural areas) that
556 vary in permeability. Human modification of landscapes, such as urban development of roads or
557 C4 plant monocultures for agriculture, can alter diet and nutrient transfer by animals (Magioli *et*
558 *al.* 2019). For example, Roe deer (*Capreolus capreolus*) in central France routinely act as
559 vectors for large quantities of artificially-introduced nitrogen, which they obtain by foraging in
560 agricultural areas, which are deposited near resting sites in forested areas (Abbas *et al.* 2012).
561 In New Mexico, USA, snow geese (*Chen caerulescens*) perform daily foraging trips from wildlife
562 refuges to agricultural areas to feed on corn and alfalfa. This nutrient translocation was shown
563 to increase phosphorous nutrient loadings up to 75% in wetland ponds (Kitchell *et al.* 1999).
564 Thus, animals can link natural areas with human modified landscapes and modify the nutrient
565 budgets of ecosystems.

566   Mechanistic models of animal vectored subsidies (Bampoh *et al.* 2019) could predict
567 how nutrient budgets of ecosystems are altered by the removal of species, such as large bodied
568 animals (Bello *et al.* 2015; Sobral *et al.* 2017), or specific individuals (i.e. elephant bulls in
569 Kruger National Park (Davies & Asner 2019)), or animal introductions (goat introduction in the
570 Galapagos (Bastille-Rousseau *et al.* 2017)). These models could identify causal links between
571 ecosystem functioning and animal mediated subsidies. Such knowledge would provide evidence
572 to rewilding initiatives aiming to restore lost ecosystem services through animal reintroductions
573 (Falcon Wilfredo & Hansen 2018; Lundgren *et al.* 2018).

574

575 **Conclusion**

576

577 Understanding how animals move through both natural and human dominated landscapes to
578 influence ecosystem properties and functions is in need of concerted analysis. To this end, we
579 have provided a methodological road map that draws together methods of analysis across
580 disciplinary fields. We show how, when combined, these can lead to integrative, coherent
581 understanding of how animal vectored subsidies drive spatial ecosystem structure and
582 functioning. It is through the integration and collaboration of disciplines that we can address and

583   understand the importance of this type of nutrient transport in a spatially explicit manner. We

584   hope that the introduced methodological roadmap will facilitate empirical studies that quantify

585   how much the fluxes of nutrients from one pool to another across landscapes can be attributed

586   to animal-vectored subsidies.

587

600

601

602

603

Figures

$$\frac{dN_i}{dt} = I - EN_i - U(N_i, P_i) + \epsilon M(P_i)$$
$$+ \chi_H \, L_H(H_i) + \chi_C \, L_C(C_i) + \gamma_H W(P_i, H_i) + \gamma_C W(H_i, C_i)$$
$$+ d_H \sum_{j=1}^{n} c_{ij}\gamma_H W(P_j, H_j) + d_C \sum_{j=1}^{n} c_{ij}\gamma_C W(H_j, C_j)$$

$$\frac{dP_i}{dt} = U(N_i, P_i) - M(P_i) - W(P_i, H_j)$$

$$\frac{dH_i}{dt} = (1 - \gamma_H) W_H(P_i, H_i) - L_H(H_i) + d_H \sum_{j=1}^{n} c_{ij}H_j - W_C(H_i, C_i)$$

$$\frac{dC_i}{dt} = (1 - \gamma_C) W_C(H_i, C_i) - L_C(C_i) + d_C \sum_{j=1}^{n} c_{ij}C_j$$
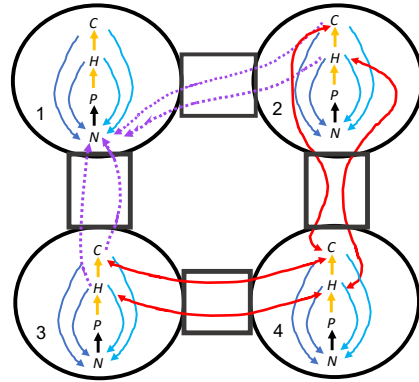
Ecosystem model component	Spatial measurements needed (sections)
Trophic interactions within and between local ecosystems	(i) The spatial extent and spatial grain size of animal movement (ii) Habitat structure shaping where animals move (iii) Available and selected resources
Nutrient translocation and deposition due to within-ecosystem carcass and nutrient deposition and between ecosystem nutrient deposition	(iv) Movement rates directional spatial flow of animals and nutrients (v) Amount of animal carcass and nutrients deposited spatially

Figure 1: Meta-ecosystem model characterizing the trophic structure and dynamics of nutrients (N), plants (P), herbivores (H) and carnivores (C) within and between four local ecosystems. In the model carnivore abundance changes as a function of assimilated intake of herbivore biomass within ecosystem i $(1 - \gamma_C)W_C(H_i, C_i)$, where γ_C is the degree of inefficiency in assimilation, loss due to natural mortality at rate $L_C(C_i)$, and gain due to migration from another local ecosystem $d_C \sum_{(j=1)} c_{ij}C_j$, where d_C is the movement rate of a carnivore and c_{ij} is the spatial connectivity between two local ecosystems (where high values reflect high connectivity and hence high ease of flow). Herbivore abundance changes as a function of assimilated intake of plant biomass $(1 - \gamma_H)W_H(P_i, H_i)$, loss due to natural mortality at rate $L_H(H_i)$, loss due to predation at rate $W_C(H_i, C_i)$ and gain due to migration from another local ecosystem $d_H \sum_{(j=1)} c_{ij}H_j$. Plant biomass changes as a function of nutrient uptake at rate $U(N_i, P_i)$, loss due to senescence at rate $M(P_i)$ and herbivory at rate $WH(P_i, H_i)$. Finally nutrient abundance changes due to global inputs I from weathering of parent geological material, release from riverine sediments, wind-born dust, or rain-driven and snowmelt-driven run-off, loss due to leaching out of the ecosystem EN_i and plant uptake at rate $U(N_i, P_i)$, and

622 additions due to recycling of plant material $\epsilon M(P_i)$, herbivore and carnivore carcasses at

623 rates $\chi_H L_H(H_i) + \chi_C L_C(C_i)$, and release of unassimilated consumption by herbivores an

624 carnivores (e.g. egesta) at rates $\gamma H W(P_i, H_i) + \gamma C W(H_i, C_i)$. Local ecosystem nutrient budgets

625 are also subsidized by unassimilated nutrient release as herbivores and carnivores migrate

626 among local ecosystems $d_H \sum_{(j=1)} c_{ij} \gamma_H W P_j, H_j) + d_C \sum_{(j=1)} c_{ij} \gamma_C W(H_j, C_j)$. These components

627 describing nutrient dynamics can ultimately be grouped according to two broad spatial

628 processes: spatial trophic interactions and spatial nutrient translocation and deposition. These

629 spatial processes can be further decomposed into five subprocesses that require different

630 methodologies to measure. A coherent picture of spatial nutrient dynamics can be developed

631 when data from the five subprocess measurements are combined into a dynamic map that

632 portrays spatial animal movement and nutrient flow in relation to the biophysical features within

633 and between local ecosystems across a landscape. Model and illustration adapted from

634 Marleau et al. (2014).

635
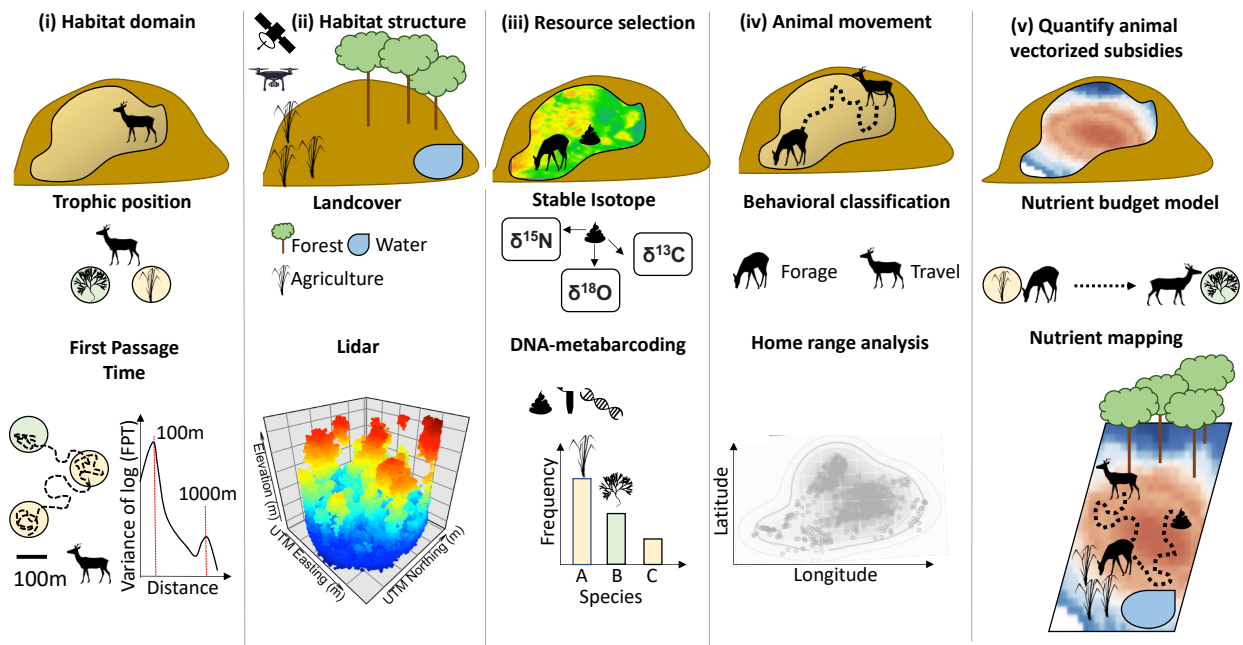
636
637 **Figure 2:** Conceptual demonstration of integrating different disciplines (sections 1,-4) for

638 quantifying animal vectorized subsidies across a landscape (section 5). (i) The habitat domain

639 helps understand the trophic position. In our hypothetical example, a roe deer (*Capreolus*

640 *capreolus*) travels across yellow patches containing agricultural areas and a green patch with

641 forested area. A first passage time analysis would reveal the scale of roe deer selection to be

642   strongest at approximately 100m. With this knowledge we can proceed on estimating the trophic

643   positions and interactions at that scale, choosing subsequent remote sensing products at the

644   same spatial scale. If we were to select a scale of 1000m – where extensive remove sensing

645   products are available (Table 1), we would see a weaker response of animals selecting their

646   environment. (ii) The habitat structure of our study region can be identified through remotely

647   sensed products, such as landcover maps. In this example, agriculture and water would be

648   convex ecosystems and likely receive abiotic inputs from forest leaves (concave ecosystem)

649   due to runoff. Convex and concave can be defined with elevation products or with Lidar to

650   obtain a 3D matrix of the environment across which animals navigate (i.e. against elevation

651   gradients during animal upslope movement). Lidar imagery was created using the rLidar and

652   rGedi packages. Habitat and environmental information (ii) can then be used as response

653   variables to understand how animals select and avoid resources and associated habitat

654   structures, using resource selection. Such resource use map is displayed in (iii) with green

655   colors indicating hotspots of habitat selection by our animal. Further, DNA-metabarcoding (iii) of

656   animal fecal matter in the study region can reveal the trophic position and the resources

657   consumed and deposited at great taxonomic detail. Understanding the stoichiometry of

658   resources consumed through stable isotopes (iii) provides insights into the composition and type

659   of nutrients that are moved by animals. (iv) Detailed information of roe deer movement obtained

660   through GPS collars reveals detailed space use of individuals (i.e. their home range) which can

661   be overlaid with the habitat structure of the landscape. Behavioural change point analysis (iv)

662   based on movement data could classify animal behaviour into foraging and travel. Coupling

663   behavioural classification and animal movement with faecal sampling for DNA-metabarcoding

664   and stable isotope can reveal sources (foraging locations) and sinks (excretion locations) of roe

665   deer-vectorized subsidies. (v) Integrating the different methodologies described, allows

666   quantifyng animal-vectorized subsidies through spatial modelling such as Stoichiometric

667   Distribution Models (section v; Leroux et al. 2017). Importantly, coupling such models with

668   abiotic nutrient deposition rates (e. g. leaching), allows us to contextualize the magnitude and

669   direction of biotic nutrient deposition rates. We could thus begin including animal vectorized

670   subsidies into ecosystem nutrient budget models (in our hypothetical case the roe deer brings

671   nutrients from the agricultural matrix into the forest ecosystem). Integrating these steps (i-v)

672   allows us to paint a picture of the landscape in which the ecological consequences of moving

673   animals are incorporated into cross-ecosystem models. Silhouettes were obtained from the

674   PhyloPic website (phylopic.org).

675

Movement   **Ecosystem**   **Sample design**   **Prediction**

Highland range (Source)

$N_{total} = N_{source}$

Migration (Translocation)

Lowland range (Recipie0nt)

$N_{tot} = N_{recip} + N_{source}$

Forage

Travel

Rest

Downslope migration

Home range

Nutrient recycling

Nutrient translocation (Highland - Lowland)

Latrine site

Drone

Manual observations

Behavioral segmentation (R)est, (F)orage, (T)ravel

C:N:P ratio
High
Low

676

Figure 3: Integration of diverse disciplines and methodologies to characterize animal-vectored subsidies; in this case nitrogen recycling and translocation by Galapagos tortoises (*Chelonoidis porteri*) in time and space. (a) Movement determines the timing and direction of animal arrival and departure of ecosystems. (b) Ecosystem nutrient budgets incorporate inputs from outside ecosystem boundaries, such as animal-vectorized subsidies. (c) Careful sample design helps elucidating drivers and predict consequences of nutrient transport by animals. Coupling large extent (remote sensing, drones) with local field measurements (manual, drones) and animal population estimates, allows (d) quantifying magnitude and flow of animal-vectorized subsidies in a spatially explicit manner and estimate what proportion of total nutrients are being mobilized by animals on the move. Tortoise silhouettes were obtained from the PhyloPic website (phylopic.org).

688
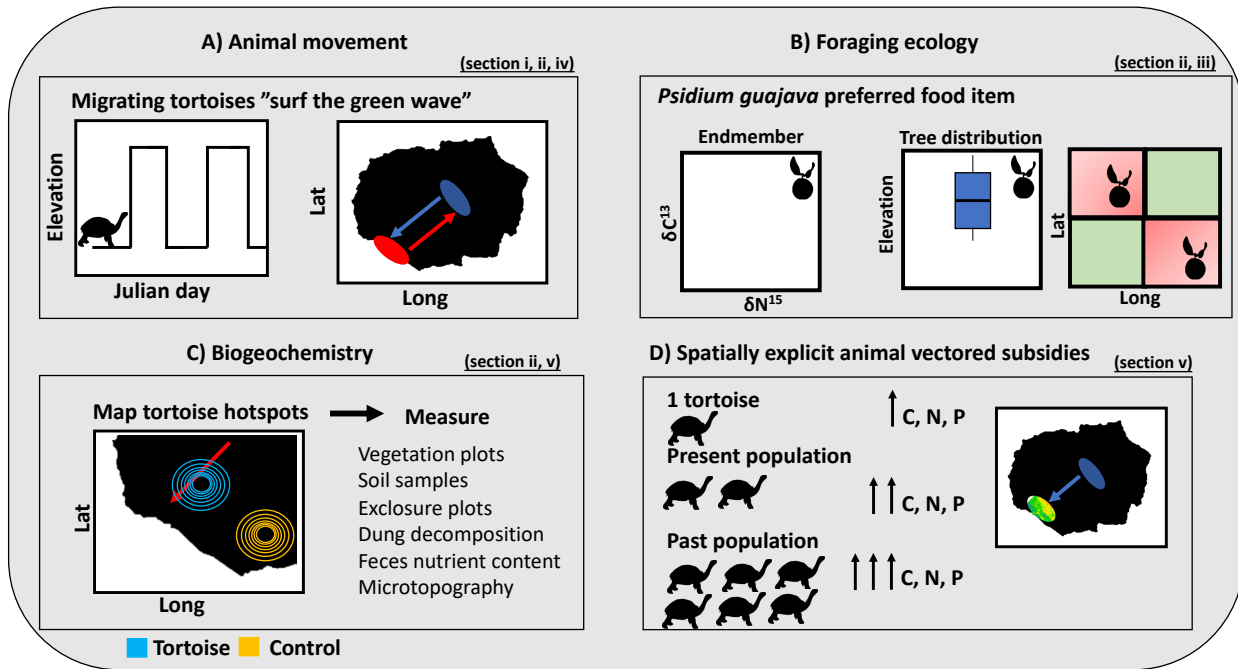
Figure 4: Conceptual example of studying nutrient transport of giant tortoises (*Chelonidis porteri*) in Santa Cruz Island. Integrating known movement patterns and foraging behaviour of this species with the distribution and nutritional composition of food items, it is possible to design an experiment to estimate the influence of tortoises transporting nutrients to the Galapagos National Park boundaries during their downslope migration. Silhouettes were obtained from the PhyloPic website (phylopic.org).
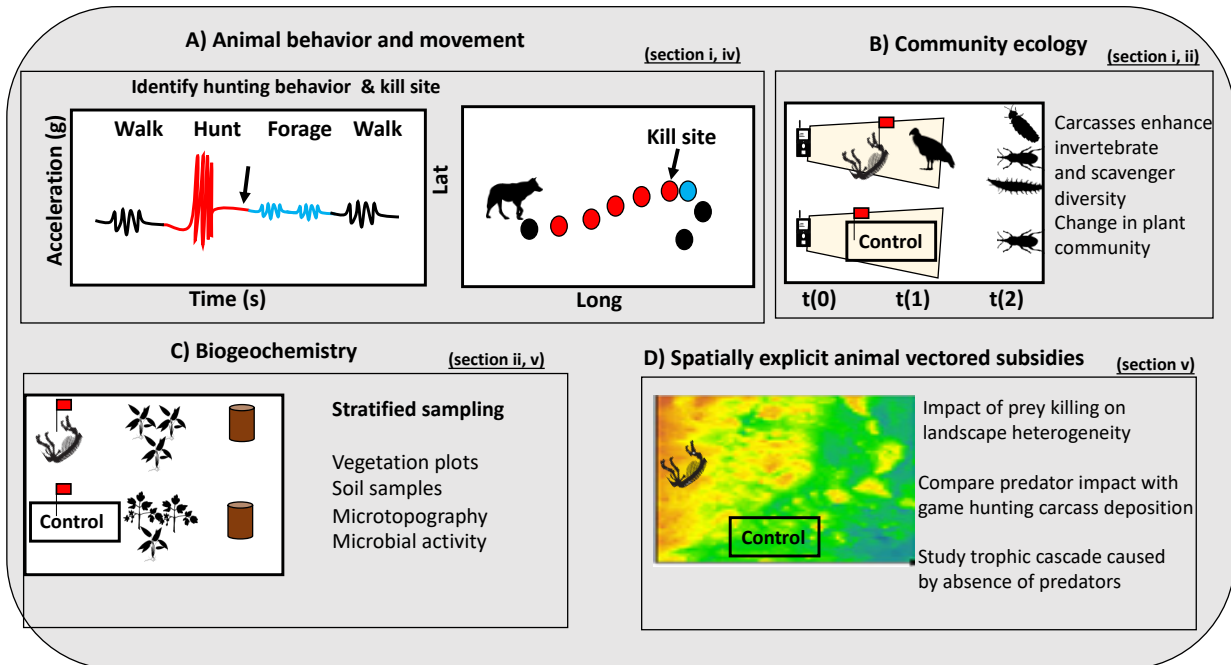
Figure 5: Conceptual example to identify killing sites of Wolfes (*Canis lupus*) with biologging technologies and quantify how predators drive landscape heterogeneity. Identifying kill sites allows studyng how carcass presence affects local biogeochemistry and community composition when compared to control locations. Silhouettes were obtained from the PhyloPic website (phylopic.org).

Table 1: Collection of applicable remote sensing products for animal mediated subsidies. We elucidate the spatio-temporal resolution and grain size of these products.

Appendix – Supplementary Material

Supplementary Material 1: Necessary code to perform movement ecology and remote sensing analysis of the Galapagos tortoise example

References

Abbas, F., Merlet, J., Morellet, N., Verheyden, H., Hewison, A.J.M., Cargnelutti, B., *et al.* (2012). Roe deer may markedly alter forest nitrogen and phosphorus budgets across Europe, 1–8.

Allan, B.M., Nimmo, D.G., Ierodiaconou, D., VanDerWal, J., Koh, L.P. & Ritchie, E.G. (2018). Futurecasting ecological research: the rise of technoecology. *Ecosphere*.

718   Allen, C.D. & Wesner, S.J. (2016). Synthesis: comparing effects of resource and consumer
719   fluxes into recipient food webs using meta- analysis. *Ecology*, 97, 594–604.
720   Amatulli, G., Domisch, S., Tuanmu, M.-N., Parmentier, B., Ranipeta, A., Malczyk, J., *et al.*
721   (2018). A suite of global, cross-scale topographic variables for environmental and
722   biodiversity modeling. *Sci. Data*, 5, 180040.
723   de Araujo Barbosa, C.C., Atkinson, P.M. & Dearing, J.A. (2015). Remote sensing of ecosystem
724   services: A systematic review. *Ecol. Indic.*, 52, 430–443.
725   Atkins, J.L., Long, R.A., Pansu, J., Daskin, J.H., Potter, A.B., Stalmans, M.E., *et al.* (2019).
726   Cascading impacts of large-carnivore extirpation in an African ecosystem. *Science (80-.).*,
727   364, 173–177.
728   Atkinson, C.L., Capps, K.A., Rugenski, A.T. & Vanni, M.J. (2017). Consumer-driven nutrient
729   dynamics in freshwater ecosystems : from individuals to ecosystems. *Biol. Rev.*, 92, 2003–
730   2023.
731   Avgar, T., Potts, J.R., Lewis, M.A. & Boyce, M.S. (2016). Integrated step selection analysis:
732   bridging the gap between resource selection and animal movement. *Methods Ecol. Evol.*,
733   7, 619–630.
734   Bampoh, D., Earl, J.E. & Zollner, P.A. (2019). Examining the relative influence of animal
735   movement patterns and mortality models on the distribution of animal transported
736   subsidies. *Ecol. Modell.*, 412, 108824.
737   Barton, P.S., McIntyre, S., Evans, M.J., Bump, J.K., Cunningham, S.A. & Manning, A.D. (2016).
738   Substantial long-term effects of carcass addition on soil and plants in a grassy eucalypt
739   woodland. *Ecosphere*, 7, e01537.
740   Bastille-Rousseau, G., Gibbs, J.P., Campbell, K., Yackulic, C.B. & Blake, S. (2017). Ecosystem
741   implications of conserving endemic versus eradicating introduced large herbivores in the
742   Galapagos Archipelago. *Biol. Conserv.*, 209, 1–10.
743   Bastille-Rousseau, G., Potts, J.R., Yackulic, C.B., Frair, J.L., Ellington, E.H. & Blake, S. (2016).
744   Flexible characterization of animal movement pattern using net squared displacement and
745   a latent state model. *Mov. Ecol.*, 4, 15.
746   Bastille-Rousseau, G., Yackulic, C., Gibbs, J., Frair, J., Cabrera, F. & Blake, S. (2019).
747   Migration triggers in a large herbivore: Galapagos giant tortoises navigating resource
748   gradients on volcanoes. *Ecology*, 100, 1–11.
749   Bauer, S. & Hoye, B.J. (2014). Migratory animals couple biodiversity and ecosystem functioning
750   worldwide. *Science (80-.).*, 344.
751   Bello, C., Galetti, M., Pizo, M.A., Magnago, L.F.S., Rocha, M.F., Lima, R.A.F., *et al.* (2015).

Defaunation affects carbon storage in tropical forests. *Sci. Adv.*, 1, e1501105.

Ben-David, M. & Flaherty, E.A. (2012). Stable isotopes in mammalian research: a beginner's guide. *J. Mammal.*, 93, 312–328.

Bennison, A., Bearhop, S., Bodey, T.W., Votier, S.C., Grecian, W.J., Wakefield, E.D., *et al.* (2018). Search and foraging behaviors from movement data: A comparison of methods. *Ecol. Evol.*, 8, 13–24.

Bergen, K.M., Goetz, S.J., Dubayah, R.O., Henebry, G.M., Hunsaker, C.T., Imhoff, M.L., *et al.* (2009). Remote sensing of vegetation 3-D structure for biodiversity and habitat: Review and implications for lidar and radar spaceborne missions. *J. Geophys. Res. Biogeosciences*, 114, G00E06.

Berzaghi, F., Verbeeck, H., Nielsen, M.R., Doughty, C.E., Bretagnolle, F., Marchetti, M., *et al.* (2018). Assessing the role of megafauna in tropical forest ecosystems and biogeochemical cycles - the potential of vegetation models. *Ecography (Cop.).*, 1934–1954.

Bidder, O.R., di Virgilio, A., Hunter, J.S., McInturff, A., Gaynor, K.M., Smith, A.M., *et al.* (2020). Monitoring canid scent marking in space and time using a biologging and machine learning approach. *Sci. Rep.*, 10, 588.

Blake, S., Guézou, A., Deem, S.L., Yackulic, C.B. & Cabrera, F. (2015). The Dominance of Introduced Plant Species in the Diets of Migratory Galapagos Tortoises Increases with Elevation on a Human-Occupied Island. *Biotropica*, 47, 246–258.

Blake, S., Wikelski, M., Cabrera, F., Guezou, A., Silva, M., Sadeghayobi, E., *et al.* (2012). Seed dispersal by Galapagos tortoises. *J. Biogeogr.*, 39, 1961–1972.

Boyce, M.S., Vernier, P.R., Nielsen, S.E. & Schmiegelow, F.K.A. (2002). Evaluating resource selection functions. *Ecol. Modell.*, 281–300.

Bracis, C., Bildstein, K.L. & Mueller, T. (2018). Revisitation analysis uncovers spatio-temporal patterns in animal movement data. *Ecography (Cop.).*, 41, 1801–1811.

Brown, D.D., Kays, R., Wikelski, M., Wilson, R. & Klimley, A.P. (2013). Observing the unwatchable through acceleration logging of animal behavior. *Anim. Biotelemetry*, 1, 1–20.

Bump, J.K., Webster, C.R., Vucetich, J.A., Peterson, R.O., Shields, J.M. & Powers, M.D. (2009a). Ungulate Carcasses Perforate Ecological Filters and Create Biogeochemical Hotspots in Forest Herbaceous Layers Allowing Trees a Competitive Advantage. *Ecosystems*, 12, 996–1007.

Bump, K.J., Rolf, O.P. & Vucetich, A.J. (2009b). Wolves modulate soil nutrient heterogeneity and foliar nitrogen by configuring the distribution of ungulate carcasses. *Ecology*, 90, 3159–3167.

786   Chapin, F.S., Matson, P.A. & Vitousek, P.M. (2012). *Principles of terrestrial ecosystem ecology*.
787   *Princ. Terr. Ecosyst. Ecol.* Springer.
788   Cherif, M. & Loreau, M. (2013). Plant-herbivore-decomposer stoichiometric mismatches and
789   nutrient cycling in ecosystems. *Proc. R. Soc. B Biol. Sci.*, 280, 20122453.
790   Clark, B.L., Bevanda, M., Aspillaga, E. & Jørgensen, N.H. (2016). Bridging disciplines with
791   training in remote sensing for animal movement: an attendee perspective. *Remote Sens.*
792   *Ecol. Conserv.*, 3, 30–37.
793   Clark, J.S., Nemergut, D., Seyednasrollah, B., Turner, P.J. & Zhang, S. (2017). Generalized
794   joint attribute modeling for biodiversity analysis: median-zero, multivariate, multifarious
795   data. *Ecol. Monogr.*, 87, 34–56.
796   Cunningham, C.X., Johnson, C.N., Barmuta, L.A., Hollings, T., Woehler, E.J. & Jones, M.E.
797   (2018). Top carnivore decline has cascading effects on scavengers and carrion
798   persistence. *Proc. R. Soc. B Biol. Sci.*, 285, 20181582.
799   Davies, A.B. & Asner, G.P. (2019). Elephants limit aboveground carbon gains in African
800   savannas. *Glob. Chang. Biol.*, 25, 1368–1382.
801   Deagle, B.E., Thomas, A.C., McInnes, J.C., Clarke, L.J., Vesterinen, E.J., Clare, E.L., *et al.*
802   (2019). Counting with DNA in metabarcoding studies: How should we convert sequence
803   reads to dietary data? *Mol. Ecol.*, 28, 391–406.
804   Dechmann, D.K.N., Wikelski, M., Ellis-Soto, D., Safi, K. & Teague O'Mara, M. (2017).
805   Determinants of spring migration departure decision in a bat. *Biol. Lett.*
806   Dirzo, R., Young, H.S., Galetti, M., Ceballos, G., Isaac, N.J.B. & Collen, B. (2014). Defaunation
807   in the Anthropocene. *Science (80-.).*
808   Doughty, C.E. (2017). Herbivores increase the global availability of nutrients over millions of
809   years. *Nat. Ecol. Evol.*, 1, 1820–1827.
810   Doughty, C.E., Roman, J., Faurby, S., Wolf, A., Haque, A., Bakker, E.S., *et al.* (2016). Global
811   nutrient transport in a world of giants. *Proc. Natl. Acad. Sci. U. S. A.*, 113, 868–73.
812   Durán, S.M., Martin, R.E., Díaz, S., Maitner, B.S., Malhi, Y., Salinas, N., *et al.* (2019). Informing
813   trait-based ecology by assessing remotely sensed functional diversity across a broad
814   tropical temperature gradient. *Sci. Adv.*, 5, eaaw8114.
815   Earl, J.E. & Zollner, P.A. (2017). Advancing research on animal-transported subsidies by
816   integrating animal movement and ecosystem modelling. *J. Anim. Ecol.*, 86, 987–997.
817   Edelhoff, H., Signer, J. & Balkenhol, N. (2016). Path segmentation for beginners: An overview of
818   current methods for detecting changes in animal movement patterns. *Mov. Ecol.*, 4.
819   Ellis-Felege, S.N., Burnam, J.S., Palmer, W.E., Sisson, D.C., Wellendorf, S.D., Thornton, R.P.,

820   *et al.* (2008). Cameras Identify White-tailed Deer Depredating Northern Bobwhite Nests.

821   *Southeast. Nat.*, 7, 562–564.

822   Ellis-Soto, D., Blake, S., Soultan, A., Guézou, A., Cabrera, F. & Lötters, S. (2017). Plant species

823   dispersed by Galapagos tortoises surf the wave of habitat suitability under anthropogenic

824   climate change. *PLoS One*, 12, e0181333.

825   Ellis-Soto, D., Merow, C., Amatulli, G., Parra, J.L. & Jetz, W. (n.d.). Continental-scale 1km

826   hummingbird diversity derived from fusing point records with lateral and elevational expert

827   information. *Ecography (Cop.).*, in review.

828   Ellis Soto, D. (2020). Giant tortoises connecting terrestrial and freshwater ecosystems in Santa

829   Cruz Island. In: *Galapagos Giant Tortoises* (eds. Gibbs, J.P., Cayot, L.J. & Tapia, W.).

830   Elsevier, Amsterdam, p. 286.

831   Falcon Wilfredo & Hansen, D.M. (2018). Island rewilding with giant tortoises in an era of climate

832   change.

833   Fauchald, P. & Tveraa, T. (2003). USING FIRST-PASSAGE TIME IN THE ANALYSIS OF

834   AREA-RESTRICTED SEARCH AND HABITAT SELECTION. *Ecology*, 84, 282–288.

835   Fleming, C.H., Fagan, W.F., Mueller, T., Olson, K.A., Leimgruber, P. & Calabrese, J.M. (2015).

836   Rigorous home range estimation with movement data: a new autocorrelated kernel density

837   estimator. *Ecology*, 96, 1182–1188.

838   Fortin, D., Beyer, H.L., Boyce, M.S., Smith, D.W., Duchesne, T. & Mao, J.S. (2005). Wolves

839   influence elk movements: Behavior shapes a trophic cascade in Yellowstone National

840   Park. *Ecology*.

841   Garriga, J., Palmer, J.R.B., Oltra, A. & Bartumeus, F. (2016). Expectation-Maximization Binary

842   Clustering for Behavioural Annotation. *PLoS One*, 11, e0151984.

843   Gibbs, J.P., Sterling, E.J. & Zabala, F.J. (2010). Giant tortoises as ecological engineers: A long-

844   term quasi-experiment in the Gal??pagos Islands. *Biotropica*, 42, 208–214.

845   Gounand, I., Harvey, E., Little, C.J. & Altermatt, F. (2018a). Meta-Ecosystems 2.0: Rooting the

846   Theory into the Field. *Trends Ecol. Evol.*, 33, 36–46.

847   Gounand, I., Little, C.J., Harvey, E. & Altermatt, F. (2018b). Cross-ecosystem carbon flows

848   connecting ecosystems worldwide. *Nat. Commun.*, 9, 4825.

849   Hancock, S., Hofton, M., Sun, X., Tang, H., Kellner, J.R., Armston, J., *et al.* (2019). The GEDI

850   simulator: A large-footprint waveform lidar simulator for calibration and validation of

851   spaceborne missions. *Earth Sp. Sci.*, 294–310.

852   Hays, G.C., Bailey, H., Bograd, S.J., Bowen, W.D., Campagna, C., Carmichael, R.H., *et al.*

853   (2019). Translating Marine Animal Tracking Data into Conservation Policy and

854   Management. *Trends Ecol. Evol.*, xx, 1–15.

855   Hirt, M.R., Grimm, V., Li, Y., Rall, B.C., Rosenbaum, B. & Brose, U. (2018). Bridging Scales:

856   Allometric Random Walks Link Movement and Biodiversity Research. *Trends Ecol. Evol.*,

857   33, 701–712.

858   Hobson, K.A., Wassenaar, L.I., Bowen, G.J., Courtiol, A., Trueman, C.N., Voigt, C.C., *et al.*

859   (2019). Chapter 10 - Outlook for Using Stable Isotopes in Animal Migration Studies. In:

860   *Tracking Animal Migration with Stable Isotopes (Second Edition)* (eds. Hobson, K.A. &

861   Wassenaar, L.I.). Academic Press, pp. 237–244.

862   Holtgrieve, G.W., Schindler, D.E. & Jewett, P.K. (2009). Large predators and biogeochemical

863   hotspots: Brown bear (Ursus arctos) predation on salmon alters nitrogen cycling in riparian

864   soils. *Ecol. Res.*

865   Hui, F.K.C. (2016). boral – Bayesian Ordination and Regression Analysis of Multivariate

866   Abundance Data in r. *Methods Ecol. Evol.*, 7, 744–750.

867   Hunter, E.A., Gibbs, J.P., Cayot, L.J., Tapia, W., Quinzin, M.C., Miller, J.M., *et al.* (2020).

868   Seeking compromise across competing goals in conservation translocations: The case of

869   the 'extinct' Floreana Island Galapagos giant tortoise. *J. Appl. Ecol.*, 57, 136–148.

870   Itow, S. (2003). Zonation Pattern, Succession Process and Invasion by Aliens in Species-poor

871   Insular Vegetation of the Galápagos Islands. *Glob. Environ. Res.*, 7, 39–58.

872   Jetz, W., Cavender-Bares, J., Pavlick, R., Schimel, D., Davis, F.W., Asner, G.P., *et al.* (2016).

873   Monitoring plant functional diversity from space. *Nat. Plants*, 2, 16024.

874   Johnson, D.H. (1980). The comparision of usage and availability measurements for evaluating

875   resource preference. *Ecology*, 61.

876   Joo, R., Boone, M.E., Clay, T.A. & Patrick, S.C. (2019). Navigating through the R packages for

877   movement, 1–29.

878   Joseph, K.B., Rolf, O.P. & John, A.V. (2009). Wolves modulate soil nutrient heterogeneity and

879   foliar nitrogen by configuring the distribution of ungulate carcasses. *Ecology*, 90, 3159–

880   3167.

881   Kartzinel, T.R., Chen, P.A., Coverdale, T.C., Erickson, D.L., Kress, W.J., Kuzmina, M.L., *et al.*

882   (2015). DNA metabarcoding illuminates dietary niche partitioning by African large

883   herbivores. *Proc. Natl. Acad. Sci.*, 112, 8019–8024.

884   Kays, R., Crofoot, M.C., Jetz, W. & Wikelski, M. (2015). Terrestrial animal tracking as an eye on

885   life and planet. *Science (80-.).*, 348, aaa2478.

886   Kelson, S.J., Power, M.E., Finlay, J.C. & Carlson, S.M. (2020). Partial migration alters

887   population ecology and food chain length: evidence from a salmonid fish. *Ecosphere*, 11,

888   e03044.

889   Kie, J.G., Matthiopoulos, J., Fieberg, J., Powell, R.A., Cagnacci, F., Mitchell, M.S., *et al.* (2010).

890   The home-range concept: are traditional estimators still relevant with modern telemetry

891   technology? *Philos. Trans. R. Soc. B Biol. Sci.*, 365, 2221–2231.

892   Kitchell, J.F., Schindler, D.E., Herwig, B.R., Post, D.M., Olson, M.H. & Oldham, M. (1999).

893   Nutrient cycling at the landscape scale: The role of diel foraging migrations by geese at the

894   Bosque del Apache National Wildlife Refuge, New Mexico. *Limnol. Oceanogr.*

895   Kleyheeg, E., Fiedler, W., Safi, K., Waldenström, J., Wikelski, M. & van Toor, M.L. (2019). A

896   Comprehensive Model for the Quantitative Estimation of Seed Dispersal by Migratory

897   Mallards. *Front. Ecol. Evol.*, 7, 1–14.

898   Knyazikhin, Y., Schull, M.A., Stenberg, P., Mõttus, M., Rautiainen, M., Yang, Y., *et al.* (2013).

899   Hyperspectral remote sensing of foliar nitrogen content. *Proc. Natl. Acad. Sci.*, 110, E185--

900   E192.

901   Kristensen, D.K., Kristensen, E., Forchhammer, M.C., Michelsen, A. & Schmidt, N.M. (2011).

902   Arctic herbivore diet can be inferred from stable carbon and nitrogen isotopes in C3 plants,

903   faeces, and wool. *Can. J. Zool.*, 89, 892–899.

904   Laso, F.J., Ben, L., Rivas-torres, G., Sampedro, C. & Arce-nazario, J. (2019). Land Cover

905   Classification of Complex Agroecosystems in the Non-Protected Highlands of the

906   Galapagos Islands.

907   Leroux, S.J., Hawlena, D. & Schmitz, O.J. (2012). Predation risk, stoichiometric plasticity and

908   ecosystem elemental cycling. *Proc. R. Soc. B Biol. Sci.*, 279, 4183–4191.

909   Leroux, S.J. & Loreau, M. (2008). Subsidy hypothesis and strength of trophic cascades across

910   ecosystems. *Ecol. Lett.*, 11, 1147–1156.

911   Leroux, S.J. & Loreau, M. (2012). Dynamics of Reciprocal Pulsed Subsidies in Local and Meta-

912   Ecosystems. *Ecosystems*, 15, 48–59.

913   Leroux, S.J., Wal, E. Vander, Wiersma, Y.F., Charron, L., Ebel, J.D., Ellis, N.M., *et al.* (2017).

914   Stoichiometric distribution models: ecological stoichiometry at the landscape extent. *Ecol.*

915   *Lett.*, 20, 1495–1506.

916   Lindeman, R.L. (1942). The Trophic-Dynamic Aspect of Ecology. *Ecology*, 23, 399–417.

917   Loreau, M. & Holt, R.D. (2004). Spatial Flows and the Regulation of Ecosystems. *Am. Nat.*, 163,

918   606–615.

919   Loreau, M., Mouquet, N. & Holt, R.D. (2003). IDEAS AND Meta-ecosystems : a theoretical

920   framework for a spatial ecosystem ecology, 673–679.

921   Lundgren, E.J., Ramp, D., Ripple, W.J. & Wallach, A.D. (2018). Introduced megafauna are

922   rewilding the Anthropocene. *Ecography (Cop.).*, 41, 857–866.

923 Maclean, I.M.D. (2020). Predicting future climate at high spatial and temporal resolution. *Glob.*

924   *Chang. Biol.*, 26, 1003–1011.

925 Maclean, I.M.D., Mosedale, J.R. & Bennie, J.J. (2019). Microclima: An r package for modelling

926   meso- and microclimate. *Methods Ecol. Evol.*, 10.

927 Magioli, M., Moreira, M.Z., Fonseca, R.C.B., Ribeiro, M.C., Rodrigues, M.G. & Ferraz, K.M.P.M.

928   de B. (2019). Human-modified landscapes alter mammal resource and habitat use and

929   trophic structure. *Proc. Natl. Acad. Sci.*, 116, 18466–18472.

930 Mahoney, P.J. & Young, J.K. (2017). Uncovering behavioural states from animal activity and

931   site fidelity patterns. *Methods Ecol. Evol.*, 8, 174–183.

932 Marleau, J.N., Guichard, F. & Loreau, M. (2014). Meta-ecosystem dynamics and functioning on

933   finite spatial networks. *Proc. R. Soc. B Biol. Sci.*

934 Massol, F., Gravel, D., Mouquet, N., Cadotte, M.W., Fukami, T. & Leibold, M.A. (2011). Linking

935   community and ecosystem dynamics through spatial ecology. *Ecol. Lett.*, 14, 313–323.

936 McCann, K.S., Rasmussen, J.B. & Umbanhowar, J. (2005). The dynamics of spatially coupled

937   food webs. *Ecol. Lett.*, 8, 513–523.

938 Mcinturf, A.G., Pollack, L., Yang, L.H. & Spiegel, O. (2019). Vectors with autonomy : what

939   distinguishes animal-mediated nutrient transport from abiotic vectors ?

940 McLean, K.A., Trainor, A.M., Asner, G.P., Crofoot, M.C., Hopkins, M.E., Campbell, C.J., *et al.*

941   (2016). Movement patterns of three arboreal primates in a Neotropical moist forest

942   explained by LiDAR-estimated canopy structure. *Landsc. Ecol.*, 31, 1849–1862.

943 McSherry, M.E. & Ritchie, M.E. (2013). Effects of grazing on grassland soil carbon: a global

944   review. *Glob. Chang. Biol.*, 19, 1347–1357.

945 Merow, C., Allen, J.M., Aiello-Lammens, M. & Silander, J.A. (2016). Improving niche and range

946   estimates with Maxent and point process models by integrating spatially explicit

947   information. *Glob. Ecol. Biogeogr.*, 25, 1022–1036.

948 Merow, C., Wilson, A.M. & Jetz, W. (2017). Integrating occurrence data and expert maps for

949   improved species range predictions. *Glob. Ecol. Biogeogr.*, 26, 243–258.

950 Mertes, K., Jarzyna, M.A. & Jetz, W. (2020). Hierarchical multi-grain models improve

951   descriptions of species' environmental associations, distribution, and abundance. *Ecol.*

952   *Appl.*

953 Mertes, K. & Jetz, W. (2017). Disentangling scale dependencies in species environmental

954   niches and distributions. *Ecography (Cop.).*

955 Metcalf, J.L., Xu, Z.Z., Weiss, S., Lax, S., Van Treuren, W., Hyde, E.R., *et al.* (2016). Microbial

956   community assembly and metabolic function during mammalian corpse decomposition.

957   *Science (80-.)*.

958   Michelot, T. & Blackwell, P.G. (2019). State-switching continuous-time correlated random walks.

959   *Methods Ecol. Evol.*, 0, 1–13.

960   Michelot, T., Blackwell, P.G. & Matthiopoulos, J. (2019). Linking resource selection and step

961   selection models for habitat preferences in animals. *Ecology*, 100, e02452.

962   Montagano, L., Leroux, S.J., Giroux, M.-A. & Lecomte, N. (2019). The strength of ecological

963   subsidies across ecosystems: a latitudinal gradient of direct and indirect impacts on food

964   webs. *Ecol. Lett.*, 22, 265–274.

965   Nathan, R., Getz, W.M., Revilla, E., Holyoak, M., Kadmon, R., Saltz, D., *et al.* (2008). A

966   movement ecology paradigm for unifying organismal movement research Ran. *Pnas*, 105,

967   19052–19059.

968   Nathan, R., Spiegel, O., Fortmann-Roe, S., Harel, R., Wikelski, M. & Getz, W.M. (2012). Using

969   tri-axial acceleration data to identify behavioral modes of free-ranging animals: general

970   concepts and tools illustrated for griffon vultures. *J. Exp. Biol.*, 215, 986–96.

971   Newsome, S.D., Clementz, M.T. & Koch, P.L. (2010). Using stable isotope biogeochemistry to

972   study marine mammal ecology. *Mar. Mammal Sci.*, 26, 509–572.

973   Pansu, J., Guyton, J.A., Potter, A.B., Atkins, J.L., Daskin, J.H., Wursten, B., *et al.* (2019).

974   Trophic ecology of large herbivores in a reassembling African ecosystem. *J. Ecol.*, 107,

975   1355–1376.

976   Patterson, T.A., Thomas, L., Wilcox, C., Ovaskainen, O. & Matthiopoulos, J. (2008).

977   State–space models of individual animal movement. *Trends Ecol. Evol.*, 23, 87–

978   94.

979   Perrig, P.L., Donadio, E., Middleton, A.D. & Pauli, J.N. (2017). Puma predation subsidizes an

980   obligate scavenger in the high Andes. *J. Appl. Ecol.*, 54, 846–853.

981   Pettorelli, N., Laurance, W.F., O'Brien, T.G., Wegmann, M., Nagendra, H. & Turner, W. (2014).

982   Satellite remote sensing for applied ecologists: Opportunities and challenges. *J. Appl.*

983   *Ecol.*, 51, 839–848.

984   Pettorelli, N., to Bühne, H., Tulloch, A., Dubois, G., Macinnis-Ng, C., Queirós, A.M., *et al.*

985   (2018). Satellite remote sensing of ecosystem functions: opportunities, challenges and way

986   forward. *Remote Sens. Ecol. Conserv.*, 4, 71–93.

987   Picardi, S., Smith, B.J., Boone, M.E., Frederick, P.C., Cecere, J.G., Rubolini, D., *et al.* (2019). A

988   data-driven method to locate nest sites and estimate reproductive outcome from avian

989   telemetry data. *bioRxiv*, 562025.

990 Pollock, L.J., Tingley, R., Morris, W.K., Golding, N., O'Hara, R.B., Parris, K.M., *et al.* (2014).
991   Understanding co-occurrence by modelling species simultaneously with a Joint Species
992   Distribution Model (JSDM). *Methods Ecol. Evol.*, 5, 397–406.
993 Post, D.M. (2002). Using stable isotopes to estimate trophic position: Models, methods, and
994   assumptions. *Ecology*.
995 Remelgado, R., Leutner, B., Safi, K., Sonnenschein, R., Kuebert, C. & Wegmann, M. (2017).
996   Linking animal movement and remote sensing - mapping resource suitability from a remote
997   sensing perspective. *Remote Sens. Ecol. Conserv.*, 1–14.
998 Remelgado, R., Wegmann, M. & Safi, K. (2019). rsmove —An r package to bridge remote
999   sensing and movement ecology . *Methods Ecol. Evol.*
1000 Ripple, W.J., Estes, J.A., Beschta, R.L., Wilmers, C.C., Ritchie, E.G., Hebblewhite, M., *et al.*
1001   (2014). Status and Ecological Effects of the World's Largest Carnivores. *Science (80-.).*,
1002   343, 1241484.
1003 Risch, A.C., Frossard, A., Schütz, M., Frey, B., Morris, A.W. & Bump, J.K. (2020). Effects of elk
1004   and bison carcasses on soil microbial communities and ecosystem functions in
1005   Yellowstone, USA. *Funct. Ecol.*, 00, 1–12.
1006 Rivas-Torres, G.F., Benítez, F.L., Rueda, D., Sevilla, C. & Mena, C.F. (2018). A methodology
1007   for mapping native and invasive vegetation coverage in archipelagos: An example from the
1008   Galápagos Islands. *Prog. Phys. Geogr.*
1009 Sage, R.F. & Zhu, X.-G. (2011). Exploiting the engine of C(4) photosynthesis. *J. Exp. Bot.*
1010 Schmitz, O.J., Hawlena, D. & Trussell, G.C. (2010). Predator control of ecosystem nutrient
1011   dynamics. *Ecol. Lett.*
1012 Schmitz, O.J., Miller, J.R.B., Trainor, A.M. & Abrahms, B. (2017). Toward a community ecology
1013   of landscapes: predicting multiple predator–prey interactions across geographic space.
1014   *Ecology*, 98, 2281–2292.
1015 Schmitz, O.J., Rosenblatt, A.E. & Smylie, M. (2016). Temperature dependence of predation
1016   stress and the nutritional ecology of a generalist herbivore. *Ecology*, 97, 3119–3130.
1017 Schmitz, O.J., Wilmers, C.C., Leroux, S.J., Doughty, C.E., Atwood, T.B., Galetti, M., *et al.*
1018   (2018). Animals and the zoogeochemistry of the carbon cycle. *Science (80-.).*, 362,
1019   eaar3213.
1020 Schneider, F.D., Morsdorf, F., Schmid, B., Schimel, D.S., Schaepman, M.E., Petchey, O.L., *et*
1021   *al.* (2017). Mapping functional diversity from remotely sensed morphological and
1022   physiological forest traits. *Nat. Commun.*, 8.
1023 Sitters, J., Atkinson, C.L., Guelzow, N., Kelly, P. & Sullivan, L.L. (2015). Spatial stoichiometry:

1024   Cross-ecosystem material flows and their impact on recipient ecosystems and organisms.
1025   *Oikos*, 124, 920–930.
1026   Sobral, M., Silvius, K.M., Overman, H., Oliveira, L.F.B., Raab, T.K. & Fragoso, J.M.V. (2017).
1027   Mammal diversity influences the carbon cycle through trophic interactions in the Amazon.
1028   *Nat. Ecol. Evol.*, 1, 1670–1676.
1029   Somveille, M., Manica, A. & Rodrigues, A.S.L. (2019). Where the wild birds go: explaining the
1030   differences in migratory destinations across terrestrial bird species, 225–236.
1031   Somveille, M., Rodrigues, A.S.L. & Manica, A. (2018). Energy efficiency drives the global
1032   seasonal distribution of birds. *Nat. Ecol. Evol.*, 2, 962–969.
1033   Strandburg-Peshkin, A., Farine, D.R., Couzin, I.D. & Crofoot, M.C. (2015). Shared decision-
1034   making drives collective movement in wild baboons. *Science (80-.).*, 348, 1358–1361.
1035   Strandburg-Peshkin, A., Farine, D.R., Crofoot, M.C. & Couzin, I.D. (2017). Habitat and social
1036   factors shape individual decisions and emergent group structure during baboon collective
1037   movement. *Elife*, 6.
1038   Stuart, M.B., McGonigle, A.J.S. & Willmott, J.R. (2019). Hyperspectral Imaging in Environmental
1039   Monitoring: A Review of Recent Developments and Technological Advances in Compact
1040   Field Deployable Systems. *Sensors (Basel).*, 19, 3071.
1041   Subalusky, A.L., Dutton, C.L., Rosi-Marshall, E.J. & Post, D.M. (2015). The hippopotamus
1042   conveyor belt: vectors of carbon and nutrients from terrestrial grasslands to aquatic
1043   systems in sub-Saharan Africa. *Freshw. Biol.*, 60, 512–525.
1044   Subalusky, A.L., Dutton, C.L., Rosi, E.J. & Post, D.M. (2017). Annual mass drownings of the
1045   Serengeti wildebeest migration influence nutrient cycling and storage in the Mara River.
1046   *Proc. Natl. Acad. Sci.*, 114, 7647 LP-7652.
1047   Subalusky, A.L. & Post, D.M. (2018). Context dependency of animal resource subsidies. *Biol.*
1048   *Rev.*
1049   Thorson, J.T., Scheuerell, M.D., Shelton, A.O., See, K.E., Skaug, H.J. & Kristensen, K. (2015).
1050   Spatial factor analysis: a new tool for estimating joint species distributions and correlations
1051   in species range. *Methods Ecol. Evol.*, 6, 627–637.
1052   van Toor, M.L., O'Mara, M.T., Abedi-Lartey, M., Wikelski, M., Fahr, J. & Dechmann, D.K.N.
1053   (2019). Linking colony size with quantitative estimates of ecosystem services of African
1054   fruit bats. *Curr. Biol.*, 29, R237–R238.
1055   Tsalyuk, M., Kilian, W., Reineking, B. & Getz, W.M. (2019). Temporal variation in resource
1056   selection of African elephants follows long-term variability in resource availability. *Ecol.*
1057   *Monogr.*, 89, e01348.

1058 Tucker, M.A., Böhning-Gaese, K., Fagan, W.F., Fryxell, J.M., Van Moorter, B., Alberts, S.C., *et*
1059 *al.* (2018). Moving in the Anthropocene: Global reductions in terrestrial mammalian
1060 movements. *Science (80-.).*

1061 Vanni, M.J. (2002). N UTRIENT C YCLING B Y A NIMALS IN F RESHWATER E COSYSTEMS.

1062 Wang, Y., Nickel, B., Rutishauser, M., Bryce, C.M., Williams, T.M., Elkaim, G., *et al.* (2015).
1063 Movement, resting, and attack behaviors of wild pumas are revealed by tri-axial
1064 accelerometer measurements. *Mov. Ecol.*, 3, 2.

1065 Weathers, K.C., Strayer, D.L. & Likens, G.E. (2012). *Fundamentals of ecosystem science*.
1066 *Fundam. Ecosyst. Sci.*

1067 Wegmann, M. (2017). Remote Sensing Training in Ecology and Conservation – challenges and
1068 potential. *Remote Sens. Ecol. Conserv.*, 3, 5–6.

1069 Wenger, S.J., Subalusky, A.L. & Freeman, M.C. (2019). The missing dead: The lost role of
1070 animal remains in nutrient cycling in North American Rivers. *Food Webs*, 18, e00106.

1071 West, J.B., Bowen, G.J., Dawson, T.E. & Tu, K.P. (2010). *Isoscapes: Understanding movement,*
1072 *pattern, and process on earth through isotope mapping. Isoscapes Underst. Movement,*
1073 *Pattern, Process Earth Through Isot. Mapp.*

1074 Wilcove, D.S. & Wikelski, M. (2008). Going, Going, Gone: Is Animal Migration Disappearing.
1075 *PLoS Biol.*, 6, e188.

1076 Williams, T.M., Wolfe, L., Davis, T., Kendall, T., Richter, B., Wang, Y., *et al.* (2014).
1077 Instantaneous energetics of cougar kills reveals advantage of felid sneak attacks. *Science*
1078 *(80-.).*, 17331, 1–18.

1079 Wilmers, C.C., Nickel, B., Bryce, C.M., Smith, J.A., Wheat, R.E. & Yovovich, V. (2015). The
1080 golden age of bio-logging: how animal-borne sensors are advancing the frontiers of
1081 ecology. *Ecology*, 96, 1741–1753.

1082 Wilson, R.P., Börger, L., Holton, M.D., Scantlebury, D.M., Gómez-Laich, A., Quintana, F., *et al.*
1083 (2020). Estimates for energy expenditure in free-living animals using acceleration proxies:
1084 A reappraisal. *J. Anim. Ecol.*, 89, 161–172.

1085 Wilson, R.P., WHITE, C.R., QUINTANA, F., HALSEY, L.G., LIEBSCH, N., MARTIN, G.R., *et al.*
1086 (2006). Moving towards acceleration for estimates of activity-specific metabolic rate in free-
1087 living animals: the case of the cormorant. *J. Anim. Ecol.*, 75, 1081–1090.

1088 Winner, K., Noonan, M.J., Fleming, C.H., Olson, K.A., Mueller, T., Sheldon, D., *et al.* (2018).
1089 Statistical inference for home range overlap. *Methods Ecol. Evol.*, 9, 1679–1691.

1090 Xie, H., Luo, X., Xu, X., Pan, H. & Tong, X. (2016). Automated subpixel surface water mapping
1091 from heterogeneous urban environments using Landsat 8 OLI imagery. *Remote Sens.*, 8,

1092   1–16.

1093   Zellweger, F., Coomes, D., Frenne, P. De, Lenoir, J. & Rocchini, D. (2018). Advances in

1094   Microclimate Ecology Arising from Remote Sensing. *Trends Ecol. Evol.*, 1–15.

1095